Light Metals 2011 *Edited by: Stephen J. Lindsay*
TMS (The Minerals, Metals & Materials Society), 2011

DEVELOPMENT OF INDUSTRIAL BENCHMARK FINITE ELEMENT ANALYSIS MODEL TO STUDY ENERGY EFFICIENT ELECTRICAL CONNECTIONS FOR PRIMARY ALUMINIUM SMELTERS

D. Molenaar[1], K. Ding[2] and A. Kapoor[2]
[1] CSIRO. Melbourne, Australia.
[2] Swinburne University of Technology. Melbourne Australia

Keywords: contact resistance, contact pressure, stub to carbon voltage drop, cast iron, anode carbon, anode assembly

Abstract

Process improvements of 5 MW per plant (50,000 t CO_2e pa for coal based electricity) are possible through optimisation of the complex cast iron to carbon contacts within aluminium smelter anode and cathode assemblies. Finite element analysis is considered the tool of choice within industry for assessing potential improvements; however there are limitations with existing models regarding handling of contact resistance and carbon stress state. A study has been undertaken using thermo-electrical-mechanical finite element analysis of the cast iron to carbon contact for an anode assembly. The contact pressure and electrical resistance and its dependence on temperature have been derived from data available in the public domain. This paper presents development of the benchmark model including results. The benchmark model will be used as the reference point for the development of more advanced models in ongoing studies to assist primary aluminium smelters achieve these substantial savings in energy efficiency and reduced greenhouse gas emissions.

Introduction

Aluminium smelters operate at currents in the range of 100-400 kA DC. Most reduction cells operate at approximately 4.5 volts DC each and, as the theoretical reduction of alumina requires about 1.8 volts DC, it is clear that there are significant energy losses in the process. Of the excess 2.7 volts, power losses associated with electrical conductors and connections represent approximately 0.2-0.4 volts and a significant portion of these losses are contained within the complex cast iron to carbon contacts within aluminium smelter anode and cathode assemblies [1]. Figure 1 shows the components of a typical anode assembly used within the aluminium smelting process comprising (1) aluminium rod, (2) aluminium-titanium-steel transition joint or clad, (3) steel crossbar or yoke, (4) steel stubs, (5) cast iron thimbles and (6) carbon anode. The anode assembly shown in Figure 1 has been specifically designed for this study. Of particular interest in this paper is the electrical connection system of the steel stub to cast iron thimble to anode carbon, referred to as the stub to carbon (STC) connection.

There are generally three methods employed by industry to study potential energy efficiency savings that may be present in the anode assembly STC connection. The first has historically been to undertake extensive in-plant trials of suitably instrumented anode assemblies set into actual reduction cells and monitored over the entire period of operation [2]. The operating environment within a reduction cell offers many technical challenges to overcome in order to ensure that a measurement system is sufficiently robust and will generate valid data throughout the measurement campaign. In-plant trials are logistically demanding, expensive and labour intensive.

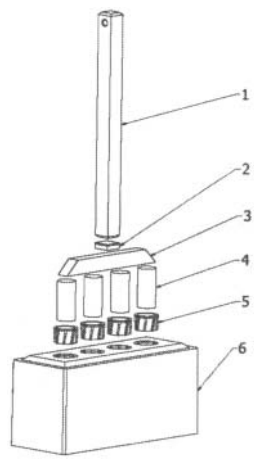

Figure 1. Components of a typical anode assembly

They require many months preparation and will generally mandate a very high number of sample repeats to form a statistically valid result due to the inherently high levels of variation within and between anode assemblies. The second method is the off-line experimental laboratory. Major issues with this approach are; (a) significantly reduced current density making it very difficult to detect small changes in contact resistance, (b) heating and protection of the anode carbon from combustion during testing and (c) it is common to employ smaller portions of an actual anode in the test rig resulting in non-representative overall geometry which will cause significant alterations to the constriction of current through the portion of carbon being tested. Also, in the latter case the smaller sized carbon may not withstand the stress generated from differential thermal expansion and will likely cause the carbon to crack, invalidating the test data. It is not practical or efficient to test entire anode assemblies in an off-line laboratory. The third approach employed is finite element analysis (FEA) and this is considered the tool of choice within industry for assessing these potential improvements [3-6]; however there are numerous limitations with existing models, the two most important ones being the handling of contact resistance and carbon stress state.

The purpose of this paper is to describe in detail the development of a benchmark finite element model using a proper analysis procedure to achieve a thermo-electrical-mechanical analysis of the cast iron to carbon contact for an anode assembly. This benchmark model will be used as the reference point for the development of more advanced models in ongoing studies towards assisting primary aluminium smelters achieve substantial savings in energy efficiency and reduced greenhouse gas emissions.

Development of Contact Resistance Relationship

To be able to utilize fully coupled thermo-electrical analysis in the finite element model, it is first necessary to define the contact resistance as a function of both temperature and contact pressure. The basis for developing the required relationships draws upon the original work undertaken by Rhedey and Castonguay [7] in which a chart is presented showing the impact on contact resistance for a steel-carbon system as a function of contact pressure. In this study the original data set was divided into three distinct pressure regions being (A) low, (B) medium and (C) high. Basic curve fitting techniques were used to define a suitable set of equations that adequately calculated the effect of contact pressure on contact resistance for all temperatures and pressures expected within the model. The following overarching set of equations was found to describe the relationship within the temperature range of interest between 0-950°C:

Region A (0.00029 MPa $\leq$ P < 2.4525 MPa)

$$CR_a=a_0*\exp(a_1*T)*(P*100/9.81)\wedge(a_2*T^2+a_3*T+a_4) \quad (1)$$

Region B (2.4525 MPa $\leq$ P $\leq$ 9.81 MPa)

$$CR_b=(b_0*T^2+b_1*T+b_2)\exp(b_3*T^2+b_4*T+b_5)(P*100/9.81) \quad (2)$$

Region C (P > 9.81 MPa)

$$CR_c=(c_0*T^2+c_1*T+c_2)\exp 100*(c_3*T^2+c_4*T+c_5) \quad (3)$$

If P < 0.00029 MPa, CR will be very high = 2000 ohm.mm^2.

Where:

T - mean temperature at the contact surface (°C)

CR_i - contact resistance (ohm.mm^2), i=a,b,c

i_0, i_1, i_2, i_3, i_4 and i_5 – material constants obtained through curve fitting

Figure 2 shows the contact resistance relationship defined by equations (1), (2) and (3) which are presented as a function of both contact pressure and temperature between 0-950°C.

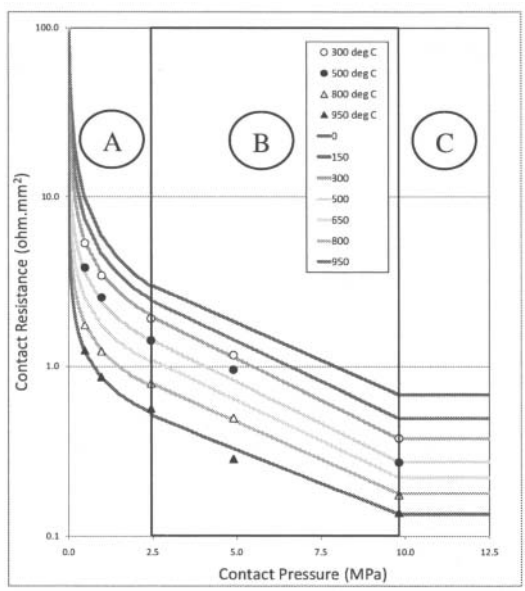

Figure 2. Chart of contact resistance relationships used in the subroutine with overlay of original data from [7]

Detailed Model Geometry

A generic three dimensional anode assembly model is constructed and run over several orders of magnitude scale, for example; the domain is approximately 3 m × 2 m as shown in Figure 3 and Figure 4, but the radii at the base of the stub hole and cast iron thimble are 3 mm as shown in Figure 5. This imposes considerable density of meshing issues at the radii to ensure that all elements maintain a proper aspect ratio and will not impact convergence.

To more accurately model the electrical and thermal conduction through weldments, the components of assemblies being joined by each weldment were separated by 1 mm to ensure electrical isolation, forcing the current to flow through all welds as is observed in reality.

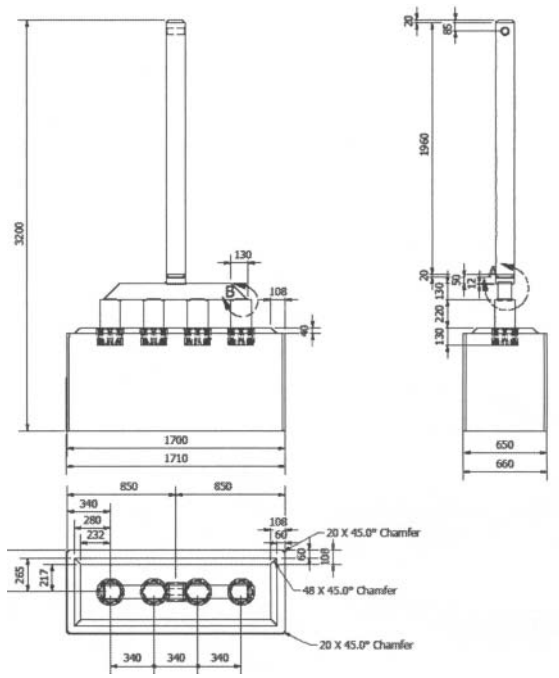

Figure 3. Full anode assembly dimensions

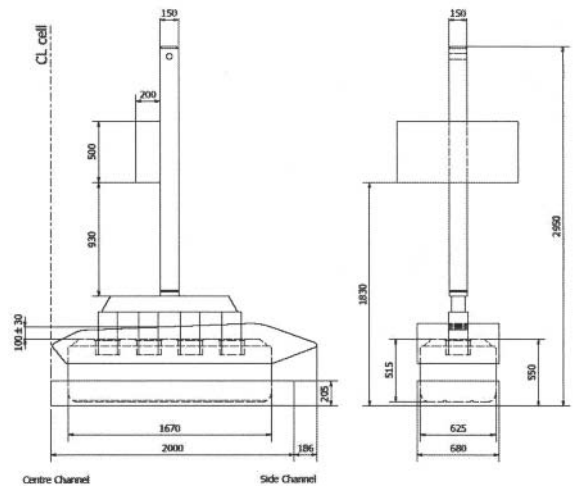

Figure 4. Key dimensions for half rota operation

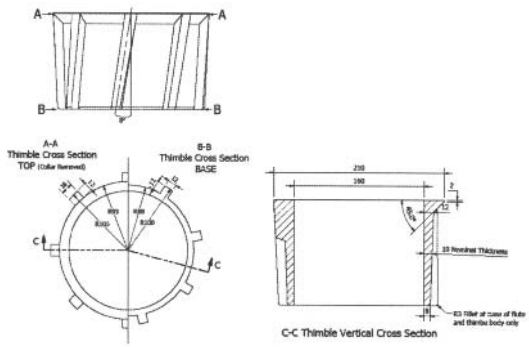

Figure 5. Cast iron thimble dimensions

Modelling Technique

The STC electrical contact resistance is defined as a set of functions of temperature and contact pressure using equations (1), (2) and (3). The functions are programmed into a user defined subroutine for the ABAQUS modelling software, which specifies the gap conductance for the STC contact surfaces. The thermo-mechanical modelling process deals with the air gap change in expansion and shrinkage and contact pressure in the STC interfaces for both the casting operation and the cell operation. In a coupled thermal-electrical modelling process, the nodal temperature becomes a known variable while the node contact pressure can be read in from an external file generated from the thermo-mechanical modelling process. This approach allows the electrical contact resistance for the STC interfaces to be automatically determined within the ABAQUS subroutine and thus no calibration or manual adjustment is required.

Modelling Flow Chart

There are three main steps in the modelling procedure, shown as the flow chart of Figure 6.

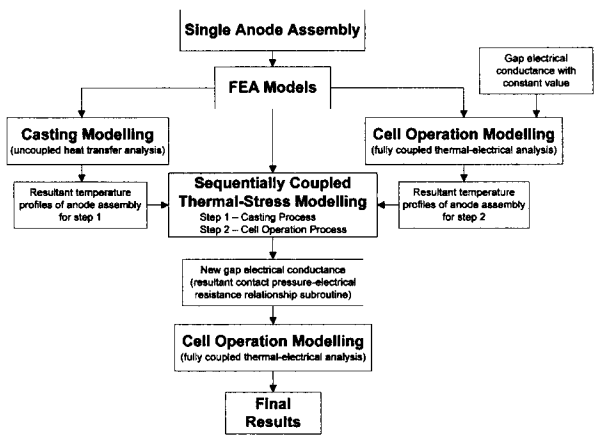

Figure 6. Flow chart of modelling procedures

Step 1: Transient thermal analysis and thermal-electrical analysis were performed to determine the temperature profiles and historic data at each node of anode assembly in the casting operation and the cell operation (at half rota), respectively;

Step 2: Thermo-mechanical analysis was undertaken to obtain the main output of contact pressures on the interfaces between cast iron thimble and carbon in the stub holes, reading the results of each nodal temperature history in the anode assembly from step 1 as the thermal inputs;

Step 3: Thermal-electrical analysis was performed using the ABAQUS user defined subroutine in terms of a function of temperature and contact pressure. The contact pressure was read from the previous thermo-mechanical analysis (step 2).

Software and Hardware

All analyses were run on a personal computer. This was done in order to assess the performance statistics of a PC available as a simple facility in the industry work environment in handling such computationally intensive tasks. The details of the computer configuration and the computational software used for this project are shown in Table I.

Table I. Computational configuration and environments

Hardware	HP Z400 6-DIMM Workstation. Intel Xeon W3580 3.33GHz CPU - 8MB of RAM
Software	ABAQUS 6.9 -EF, Microsoft Visual Studio 2008, and Intel® Visual Fortran Compiler Professional Edition 11.1 .054 for Window XP 64bits

Model Setup

The FEA model used 4 or 8 node brick continuous elements. The FEA mesh was kept the same, but the element type was in accordance with each analytical scheme. For heat transfer analyses, DC3D8 and DC3D4 (linear bricks) were used. For thermo-mechanical analyses, C3D8R and C3D4 (linear brick) were used. For thermal-electrical analyses, DC3D8E and DC3D4E (linear bricks) were used. The details of element and node numbers of the FEA model for each part are shown in Table II. The actual models are shown in Figure 7.

Table II. Details of FEA mesh model

Anode assembly parts	Element numbers	Node numbers
Hanger (Al rod, steel, weld)	25730	15646
Anode	50271	15965
Thimble (total 4)	17388	5856
Cover	9065	9126
Bath	1584	2815
Total	104038	49408

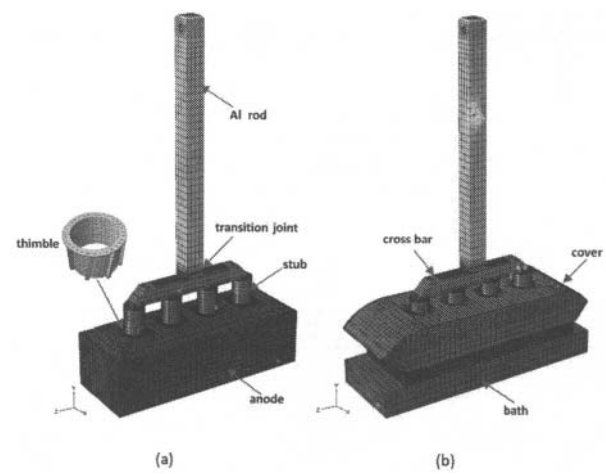

Figure 7. (a) Sequentially coupled thermo-mechanical and uncoupled heat transfer models; (b) fully coupled thermal-electrical model

Material Properties

The FEA model includes 8 kinds of materials specified as follows:

- Stub, crossbar and steel weld: SAE1020
- Aluminium rod: similar to Al6061
- Aluminium weld: similar to Al4043
- Transition joint includes three parts of material: SAE1020, Al4043 and CP-Ti
- Thimble: cast iron (grey cast iron)
- Anode carbon: baked carbon material – special C
- Cover: 50% alumina + 50% solid cryolite
- Bath: molten cryolite.

Process Parameters and Boundary Conditions

The key operational parameters are:

- Anode rod current of 7500 Amps
- Anode Cathode Distance (ACD) of 35 mm
- Bath height of 205 mm (35 + 170 mm)
- Cover height profiled at 100 ± 30 mm
- Half rota anode carbon dimensions of 1670 × 625 × 515 mm
- Bath temperature of 960 °C
- Temperature of cast iron at casting of 1450 °C

The boundary conditions for the thermo-mechanical analysis are addressed below:

- Fixed boundary conditions were applied to the side surface of Al rod where clamped to the anode beam.
- The bottom surface of the anode carbon during the thermo-mechanical analysis of the casting operation was supported by the ground, but during the cell operation, the vertical constraints on the carbon were released.
- All contacts were applied for the 'hard' contact relationship in normal direction and a small sliding relationship in tangent direction with friction coefficient of 0.2. The contact between thimble and stub was assumed as a tied contact.

Simulated Voltage and Temperature Probe Locations

Validation of the modelling will require wiring of an actual anode assembly and collecting both voltage and temperature data. This has been anticipated and so predefined locations have been established in the modelling geometry to allow reporting of key voltage and temperature data for later comparison of the actual anode assembly performance. The predefined locations for monitoring and reporting voltage and temperature data are as follows and shown in Figure 8:

- STC voltage drop from the stub 50 mm above the thimble top surface to in-line with the base of the stub hole at 70 mm out from the flute base widest point. Rotated 45 degrees away from the centre of the anode. Each of the 4 stubs from side channel (S/C) to centre channel (C/C). All voltage drops are recorded from the right hand side (RHS) of the anode when looking into the cell from the side channel.
- Middle anode temperature 100 mm deep from anode top surface. STC temperature exactly as per voltage probes but on the left hand side (LHS) of anode with the stub thermocouple in 25 mm from the surface.

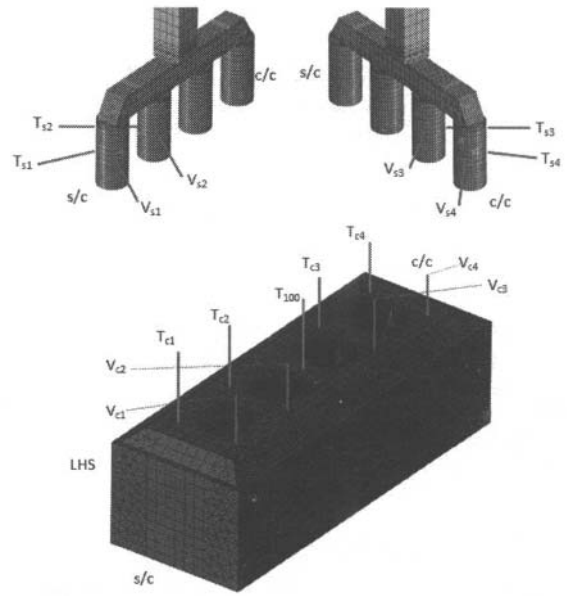

Figure 8. Simulated voltage and temperature probe locations

Modelling Results

Model Run Time Duration

Running of the model includes a very time consuming debugging process which may consume up to about 4 days to execute. This is quite a normal part of this modelling process owing to the very complex interactions between cast iron, air gap and anode carbon. Once the model has been completely debugged and convergence is possible then the final computational effort required is still quite significant in that it requires several hours to complete.

To assess the impact of using multiple CPU cores on the same machine the final computational effort was performed using 1, 2, 3 and 4 CPU cores. The results are shown in Table III.

Table III. Details of computational speed for each analysis

FEA analysis	# CPUs	Clock time (hrs)
Heat transfer analysis	1,2,3,4	0.45, 0.22, 0.17, 0.14
Thermal-electrical analysis (first pass)	1,2,3,4	0.20, 0.10, 0.06, 0.05
Thermo-mechanical analysis	1,2,3,4	2.40, 0.85, 0.66, 0.54
Thermal-electrical analysis with subroutine	1,2,3,4	0.40, 0.20, 0.15, 0.12

Temperature Profile

The resultant temperature profile for the anode assembly model is shown in Figure 9. The specific temperature probe locations data is contained in Table IV. It can be seen that the mid anode temperature at 100 mm below the carbon top surface is in the order of 560 °C by mid rota. The stubs are operating closer to 600 °C at the lower portions and around 350 °C at 50 mm above the carbon top surface. The temperature of the transition joint region is determined to be approximately 220 °C.

A parameter study was undertaken for the anode cover material thermal conductivity to establish the influence on the overall temperature profile of the STC region. A node in the middle of the anode at approximately 84 mm below the carbon top surface was utilized for this parameter study. Data are presented in Table V.

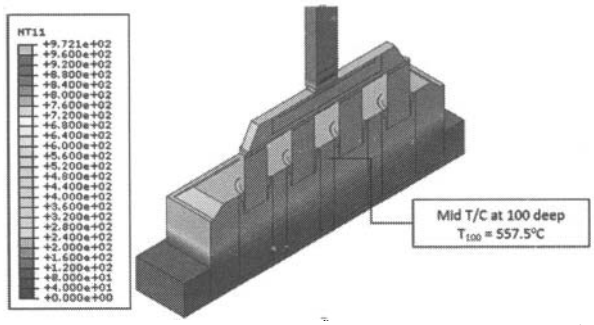

Figure 9. Temperature distribution in the anode assembly. T_{100}=557.5 °C at mid-anode and 100 mm deep

Table IV. Measured temperature points of anode carbon and stubs at mid rota

Location	Temperature [°C]	Location Descriptions
T_{100}	557.5	Mid-anode 100mm deep
T_{c1}	578.5	Near stub1, 45°, out 70mm from flute (LHS)
T_{c2}	594	Near stub2, 45°, out 70mm from flute (LHS)
T_{c3}	591	Near stub3, 45°, out 70mm from flute (LHS)
T_{c4}	577.5	Near stub4, 45°, out 70mm from flute (LHS)
T_{s1}	335.0	Stub1, 45°, up 50mm from anode surface
T_{s2}	321.0	Stub2, 45°, up 50mm from anode surface
T_{s3}	352.0	Stub3, 45°, up 50mm from anode surface
T_{s4}	358.0	Stub4, 45°, up 50mm from anode surface

Table V. Sensitivity study on anode cover thermal conductivity

Anode cover thermal conductivity (W/m.K)	T_{84} Temperature [°C]
13	514
6	549
3	591
0.5	705

Carbon Stress

The highest tensile maximum principal stress (73.7 MPa) is located at the bottom of the stub holes, specifically at the small curve of the C/C stub hole as shown in Figure 10. Parameter studies, altering only the Young's modulus (E) of cast iron and carbon materials, found a significant improvement in maximum principle stress in this region when using a low value of E. In the thermo-mechanical analysis, the highest tensile maximum principal stress predicted in the carbon anode would indicate a potential cracking problem; however, as a linear mechanical property is assumed in the model, the stress was deemed to be overestimated.

Stub Hole Contact Pressure Distribution

The resultant stub hole wall contact pressure for a middle stub is extremely low as shown in Figure 11. The values here are close to zero with only a few very discrete locations of higher stress shown around the bottom edge of the stub hole wall. However, the maximum contact pressure generated is significantly larger at 85.8 MPa for a middle stub hole and over 90 MPa for an outer stub hole.

Current Density

The current density distribution for the lower portion of the anode assembly model is shown in Figure 12. It clearly shows that the current flow is concentrated through the walls of the stub holes and not through the base.

Voltage Profile

The resultant voltage profile for the anode assembly model is shown in Figure 13. It can be seen that the lines of constant voltage distort as they approach the STC connection and that there is a very significant distortion of potential around the lower corners of the stub holes.

Voltage and Temperature Probe Location Data

The information presented in Table VI shows the voltage potential for each of the predefined locations in the anode carbon and stubs. The STC voltage drop can then be determined and is summarized in Table VII.

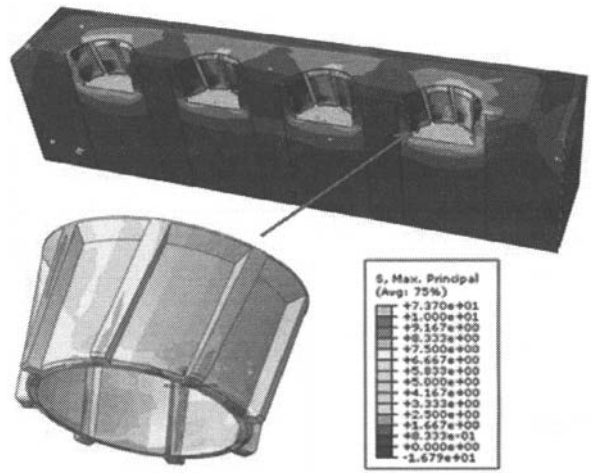

Figure 10. Maximum principal stress in the carbon anode at mid rota (Maximum value at the base of stub hole = 73.7 MPa)

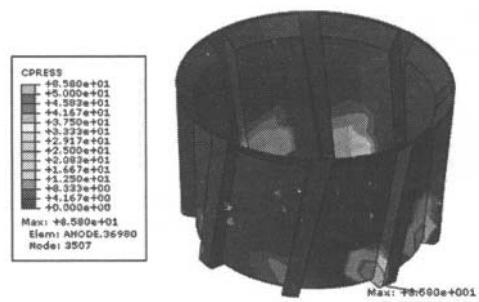

Figure 11. Contact pressure distribution in the mid stub holes at mid rota (Max. value at the base of stub hole = 85.8 MPa)

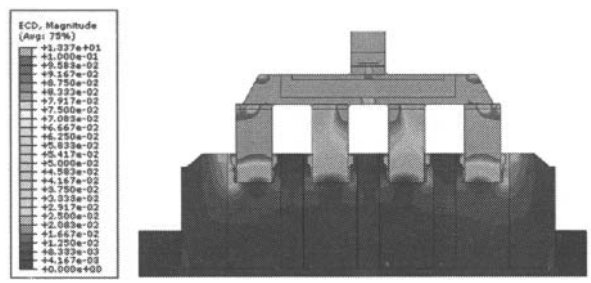

Figure 12. Current density distribution at mid rota

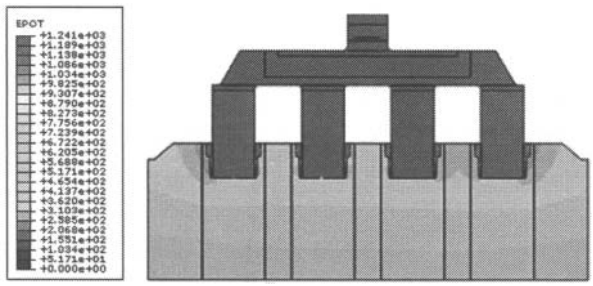

Figure 13. Voltage potential distribution at mid rota

Table VI. Measured voltage points of anode carbon and stubs at mid rota

Location	Voltage [mV]	Location Descriptions
V_{c1}	909.0	Near stub1, 45°, out 70mm from flute (RHS)
V_{c2}	901.5	Near stub2, 45°, out 70mm from flute (RHS)
V_{c3}	908.0	Near stub3, 45°, out 70mm from flute (RHS)
V_{c4}	913.5	Near stub4, 45°, out 70mm from flute (RHS)
V_{s1}	1181.0	Stub1, 45°, up 50mm from anode surface
V_{s2}	1200.0	Stub2, 45°, up 50mm from anode surface
V_{s3}	1197.0	Stub3, 45°, up 50mm from anode surface
V_{s4}	1179.0	Stub4, 45°, up 50mm from anode surface

Table VII. STC voltage drops at measured points at mid rota

Location	Voltage [mV]	Location Descriptions
$V_{STC1}(V_{s1}- V_{c1})$	272.0	Stub1 to anode near stub hole 1 at 45°
$V_{STC2}(V_{s2}- V_{c2})$	298.5	Stub2 to anode near stub hole 2 at 45°
$V_{STC3}(V_{s3}- V_{c3})$	289.0	Stub3 to anode near stub hole 3 at 45°
$V_{STC4}(V_{s4}- V_{c4})$	265.5	Stub4 to anode near stub hole 4 at 45°

Discussion

Contact Resistance Relationship

The form of equations was confirmed as suitable for the required analyses. The slight discontinuity between the pressure regions A and B is deemed to be acceptable.

Temperature Profile

Whilst the distribution of temperature throughout the anode assembly model seems quite reasonable, it does appear that the values in and around the stub holes are low. The sensitivity study conducted on the value of thermal conductivity obtained for the cover material indicates it may be too high, allowing too much heat loss to be calculated for the top of the anode assembly.

Anode Stress

The anode stress is reported as very high and would certainly exceed what could be tolerated from real anode material. The sensitivity study conducted into the Young's Modulus for both the cast iron and the anode carbon show that the resultant anode stress is sensitive to this parameter and it may be that subsequent materials testing is required to confirm these values for smelter grade materials. The over prediction of anode stress is common place for FEA modelling of this assembly and this error represents one of the two major limitations of the present modelling technique and is the topic of future study in this area.

Stub Hole Contact Pressure

It is surprising that for the bulk of the stub hole wall area the contact pressure is almost zero, furthermore that the intensity of the contact pressure at the bottom of the stub hole wall is in fact extremely large. It could well be that the low values of temperature are causing the very low contact pressures throughout the bulk of the stub hole wall, but it is presently unknown what is causing such extremely high contact pressures at the very bottom of the stub hole walls. Further investigation is required to resolve this issue.

Voltage Profile

The observed distortion of the voltage profile around the base of the stub holes is expected as it is a result of non-contact through the base of the stub holes forcing the current to flow through the walls of the stub holes. It is encouraging to see that for a four stub anode assembly that there is a relatively uniform voltage profile through the bulk of the anode. It would be expected that with fewer stubs to feed the current into the anode there would be substantially more disruption to the voltage profile in the anode. In short, a disrupted voltage profile equates to electrical inefficiency within the system.

Conclusions

This paper has discussed the successful development of a fully coupled thermo-electrical-mechanical finite element model and presented the results of this development. Further work to improve the materials properties data set relevant for this analysis is required. The benchmark model will be used as the reference point for the development of more advanced models in ongoing studies towards assisting primary aluminium smelters achieve these substantial savings in energy efficiency and reduced greenhouse gas emissions.

Acknowledgments

The authors would like to thank Dr Neal Wai Poi and CSIRO Light Metals Flagship for supporting this work and to Dr Dayalan Gunasegaram of CSIRO for trawling the public domain to provide all of the required materials properties input data. The assistance of Mr Russell Bartels of Veldor Advanced Pty Ltd is greatly appreciated in building the initial model geometry for FEA input.

References

[1] D. Molenaar, "High Amperage Electrical Connections for the Aluminium Smelting Industry" Masters thesis, Monash University, 2003.

[2] R. Peterson, "Studies of Stub to Carbon Voltage" Light Metals 1978, pp 367-378.

[3] M. Dupuis, "Development and Application of an ANSYS based thermo-electro-mechanical anode stub hole design tool", Light Metals 2010, pp 433-438.

[4] S. T.X. Hou, Q. Jiao, E. Chin, W. Crowell and C. Celik, "A numerical model for improving anode stub design in aluminium smelting process", Light Metals 1995, pp 755-761.

[5] D. Richard, P. Goulet, O. Trempe, M. Dupuis and M. Fafard, "Challenges in stub hole optimisation of cast iron rodded anodes", Light Metals 2009, pp 1067-1072.

[6] D. Richard, M. Fafard, R. Lacroix, P. Clery, Y. Maltais, "Aluminium reduction cell stub hole design using weakly coupled thermo-electro-mechanical finite element models", Finite elements in analysis and design 37, 2001, pp 287-304.

[7] P. Rhedey and L. Castonguay, "Effects of Carbonaceous Rodding Mix Formulation on Steel-Carbon Contact Resistance" Light Metals 1985, pp 1089-1105.